

Author



Small-Scale Geared Turbofan Simulation and Annular Duct Acoustics

Chen Li

Aerospace Engineering, Mechanical Engineering

Chen Li has always been fascinated with fluid dynamics and was excited by the opportunity to look into the acoustics of geared turbofans. By working on a small rotor, he was able to test a number of innovative sound-suppressing techniques without the expense and space a full-scale rotor would require. For Chen, the most satisfying part of his research was the opportunity to work, as an undergraduate, on a project at the forefront of aerospace engineering along with people who shared his passion for their work. Chen is now pursuing an M.S. in Aerospace Engineering.

Abstract

This study relates to the acoustic simulation of a realistic geared turbofan (GTF) engine, using a very-small-scale GTF from UC Irvine's Aeroacoustics Lab. The paper describes the theoretical modeling for duct acoustics of rotor-stator-interaction (RSI) inside an infinite, hard-walled annular duct with inviscid moving medium. RSI generally refers to the rotor wake interacting with the downstream stator, which then directly relates to noise emission. Bessel functions are used to compute pressure perturbations. The periodicity of the flow field is related to the specific azimuthal periodicity of the rotor, which provides the theoretical cut-off (on) criterion. Their respective acoustic properties agree rather firmly with the theoretical sound pressure level spectra plotted from actual acoustic testing. This paper is collaborated with the Aeroacoustics Lab's attempt to verify the feasibility of using small scale, stereolithographic-fabricated propellers to simulate the acoustic performance of realistic ducted fans. The developed substitute for large experimental setups could bring down experimental costs considerably and increase variation of the rotor for more innovative design. The simulator accurately reproduces the tonal noises at discrete blade passing frequencies. In the case of low-polar-angle acoustic waves, the theory successfully predicts the cut-off (on) scenarios for the first two blade-passing tones.

Faculty Mentor



The future of commercial aircraft propulsion involves turbines driving very large fans, which are essentially propellers enclosed in a duct. The so-called high-bypass turbofan engines emit distinct noise signatures that need to be attenuated for future aircraft to be extremely quiet so that they are barely perceptible to communities near airports. The paper by Mr. Chen Li explains some of the mathematics behind this noise generation. Even though the math level is above that typically taught in our undergraduate courses, a motivated undergrad like Mr. Li is able to handle the challenges and learn about the richness and beauty of things like Bessel functions. I think he had fun with it, and I hope that more undergrads will be intrigued and learn about these mathematical concepts.

Key Terms

- ◆ Annular Duct Acoustics
- ◆ Cut-Off (On) Criterion
- ◆ Rotor-Stator Interaction
- ◆ Small-Scale Geared Turbofan Simulation

Dimitri Papamoschou

Henry Samueli School of Engineering

Introduction

With rising fuel costs and various environmental concerns, aircraft engine development is tending towards very-high-bypass turbofan engines that are essentially ducted propellers (Figures 1 and 2). A prominent concept in this class of engines is the geared turbofan (GTF) engine, which features exceptional efficiency but emits noise with vexing tonal content. To conform to stringent noise regulations, the GTF engine sound emission must be understood, modeled and suppressed. Consequently, subscale experiments (1/5 of the scale of a realistic geared turbofan engine) simulating the operation of realistic ducted fans are being conducted in state-of-the-art NASA research facilities. Those experiments, however, are costly due to their large size. A similar project in the UC Irvine Aeroacoustics Lab simulates the acoustics of high-bypass turbofans with very-small-scale ducted fans (1/80 of the scale of a realistic geared turbofan engine) propelled electronically, which dramatically reduces



Figure 1

Airbus A320neo. Photo © Airbus S.A.S. 2010; computer rendering by Fixion - GWLNSD.

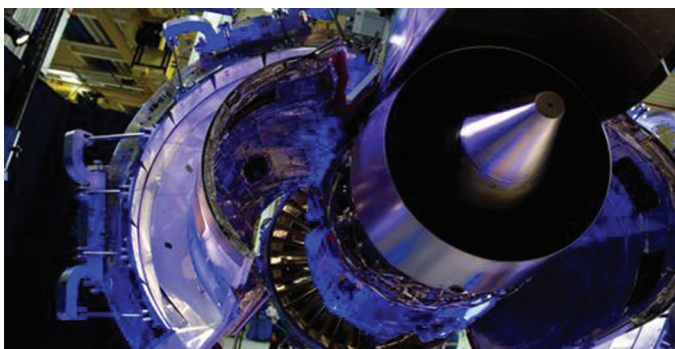


Figure 2

Next generation GTF engine designed by Pratt & Whitney

Table 1

Nomenclature for Duct Acoustics

Symbolic representations:	
B	Blade count of the rotor
c	Speed of sound inside the duct
F_m	Cut-off frequency for m
k or k_x	Axial wavenumber
$K(m,n)$	Modified radial wavenumber
m	Azimuthal periodicity
M	Mean flow Mach number
p'	Acoustic pressure (pressure perturbation)
P	Pressure
q	Inner radius of the annular duct
r	Spatial coordinate (radial direction)
R	Outer radius of the duct
s	Loading harmonic order
V	Vane count of the stator
x	Spatial coordinate (axial direction)
Z	Eigenvalue
ω	Angular Frequency
ϕ	Azimuthal angle
Ω	Angular velocity of the rotor (in rad/s)
Subscripts:	
a	BPF tone order
b or n	Radial mode order

the experimental costs. Also, due to its small size, the entire setup can be modified and produced relatively easily. The challenge to this approach is that pressure and tip velocity must be kept sufficiently large at this scale, which requires an extremely high propeller rotational speed.

This paper describes the overall design process of the rotor and the corresponding duct acoustics; it then compares the theoretical result with the acoustic data recorded in the lab.

Design of Very-Small-Scale Rotor

The primary challenge in designing very-small-scale rotors is to scale down the parameters correctly (Truong and Papamoschou, 2013). In order to keep a realistic blade tip speed and a sufficiently large fan pressure ratio while avoiding a blade stall scenario, the small blade condition demands a confined range for blade pitch angle (β) and blade solidity.

With the NACA 65 series as prototype (Truong and Papamoschou, 2013), the blade design uses open literatures on aerodynamic profile and stacking characteristics. Blade element theory (BET) is used to determine the aerody-

dynamic performance of the blade accurately. In applying the BET, the entire blade is dissected into twenty segments; each blade element encounters a different flow as they vary according to rotational speed (Ωr), angle of attack (α), pitch angle (β) and chord length (c). The model of the rotor is drafted in Solidworks and the actual rotor is 3D-printed (Figure 3).

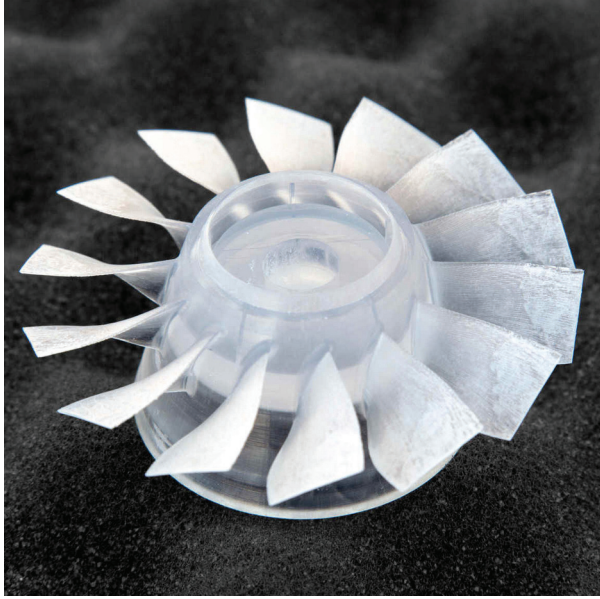


Figure 3
Stereolithographic-made rotor

Annular Duct Acoustics

This study focuses on the pressure perturbations created by rotor-stator interaction (RSI). Noises generated by this interaction range over a number of frequencies. At certain frequencies, we see distinct peaks in the sound pressure level (SPL) spectra, suggesting considerably higher noise levels. These frequencies are found to be integer multiples of the fundamental blade passing frequency (BPF):

$$\text{BPF} = B * \Omega / 2\pi \quad (1)$$

Due to the limitations of human hearing, we are only interested in the first few BPF tones. The condition at which one of them begins to propagate downstream undisturbed is called the cut-on criterion, the corresponding mode the cut-on mode; in contrast, the mode that decays exponentially along the axial direction is called the cut-off mode. How this is interrelated with the specifications of the rotor and stator largely depends on the nature of the solutions to the wave equation. The physical embodiment of this can be linked to the circumferential periodicity of the wave, which

is exemplified by the circumferential mode order m given by Equation 2a where only rotor is present, and Equation 2b where stators introduce additional periodicities. It is crucial to realize that the rotor is the object that actively creates noises; the addition of stators simply provides additional periodicities to obtain cut-off modes on a particular BPF tone.

$$m = aB \rightarrow a = 1, 2, 3 \dots \quad (2a)$$

$$m = aB + sV \rightarrow s = \dots -2, -1, 0, 1, 2 \dots \quad (2b)$$

Analytical Model

General Annular Duct Acoustics

We begin with the wave equation for the cylindrical coordinates:

$$\frac{1}{a^2} \frac{\partial^2 p'}{\partial t^2} - \left(\frac{1}{r} \frac{\partial p'}{\partial r} + \frac{\partial^2 p'}{\partial r^2} + \frac{1}{r^2} \frac{\partial^2 p'}{\partial \phi^2} + \frac{\partial^2 p'}{\partial x^2} \right) = 0 \quad (3)$$

Through separation of variables, we obtain the following expression for the pressure perturbation. $P_{(r)}$ is a real function that describes the radial dependence of pressure:

$$p' = P_{(r)} e^{i(kx + m\phi - \omega t)} \quad (4)$$

The axial wavenumber (k) in Equation 4 is crucial in determining the acoustic nature of the wave. An imaginary k can be expressed in the following way:

$$k = i|k| \quad (5)$$

According to Euler's identity, we expand the real portion of the pressure distribution as:

$$p_{real} = P_{(r)} e^{-|k|x} \cos(m\phi - \omega t) \quad (6)$$

This expression describes a wave that decays exponentially in the axial direction. It is reasonable to assume that if the duct has sufficient length the wave will be effectively evanescent and the mode associated with it is cut-off. On the other hand, with a real axial wavenumber, the real portion of the pressure distribution is given by:

$$p_{real} = P_{(r)} \cos(kx + m\phi - \omega t) \quad (7)$$

Under the assumptions of zero dissipation and hard-walled duct, we observe the unattenuated propagation of those cut-on modes. Substituting the assumed solution form for

the pressure perturbation Equation 4 into the governing wave Equation 3 yields:

$$\frac{\partial^2 P}{\partial r^2} + \frac{1}{r} \frac{\partial P}{\partial r} - \left(K^2 - \frac{m^2}{r^2} \right) P = 0 \quad (8)$$

Where K is defined as the modified wavenumber, which is discussed later.

An ordinary differential equation taking the form of Equation 8 is known as the Bessel equation (Hongbin 12). Its general solution consists of two linearly independent solutions: Bessel function of the first type, (J_m), and Bessel function of the second type, (Y_m). The general solution to Equation 8 is the linear combination of the two Bessel functions, where A_m and B_m are arbitrary constants:

$$P(r) = A_m J_m(Kr) + B_m Y_m(Kr) \quad (9)$$

The annular duct can be modeled by introducing two boundaries conditions (Equations 10a and 10b, respectively) imposed by the inner and outer walls:

$$\left(\frac{\partial P}{\partial r} \right)_{r=R} = 0 \quad (10a)$$

$$\left(\frac{\partial P}{\partial r} \right)_{r=q} = 0 \quad (10b)$$

If we insert the two boundary conditions into the solution of the wave equation and eliminate the two arbitrary constants A_m and B_m , we end up with the following expression:

$$F(KR) = J_m'(KR)Y_m'(Kq/R) - Y_m'(KR)J_m'(Kq/R) = 0 \quad (11)$$

Here we apply an additional assumption “ $R = 1$ ”; this is to normalize our analysis. This assumption cannot alter the results because the important factor is the ratio of the outer radius to the inner radius, not their absolute magnitudes.

Using Newton’s iteration method, we view the above equation as a function of K , naming it $F(K)$ (the argument is K since $R = 1$). For simplicity, we use the recurrence relation to recast $F(K)$ in terms of the Bessel Functions

$$F(K) = 0.25 [Y_{m-1}(KR) - (Y_{m+1}(KR))][Y_{m-1}(Kq/R) - Y_{m+1}(Kq/R)] - 0.25 [J_{m-1}(Kq/R) - J_{m+1}(Kq/R)][Y_{m-1}(KR) - Y_{m+1}(KR)] \quad (12)$$

The corresponding MATLAB code “Bessel_With_Roots.m” is included found in the package.

Adding the Effect of Mean Flow

In the study where a uniform mean flow is present, Equation 8 retains its form but the effect of the free stream Mach number (M) is absorbed in the following expression for the modified radial wavenumber K (Rienstra and Hirschberg, 2004):

$$K^2 = \left(\frac{\omega}{c} - Mk \right)^2 - k^2 \quad (13)$$

This introduces complexity in analyzing the propagation modes because we do not have “clear cuts” for the axial wavenumber. This is because the axial wavenumber is constituted by a real portion and a portion under the radical, which makes it possible for it to take on complex values. We rearrange Equation 13 to obtain the expression for the axial wavenumber:

$$k^\pm = \frac{-\frac{\omega}{c}M \pm \sqrt{\left(\frac{\omega}{c}\right)^2 - (1-M^2)K^2}}{1-M^2} \quad (14)$$

We also have the angular frequency of the rotor as the following:

$$\omega = aB\Omega \quad (15)$$

In a variety of literature, cut-on modes correspond to waves that propagate unattenuated (John and Lavergne, 2003), which implies purely real axial wavenumbers. As a result, examining the sign of the portion inside the radical would be sufficient to determine the acoustic nature of the mode. Consequently, the new cut-on criterion becomes the following:

$$M_{ip} > \frac{Z_{mb}}{aB} \sqrt{(1-M^2)} \quad (16)$$

A MATLAB routine named “Annular_Duct_with_Mean_Flow.m” is included in the package.

Rotor-Stator Interaction

The additional boundary conditions imposed by the stator vanes are manifested in the new expression for azimuthal periodicity m :

$$m = aB + sV \quad (17)$$

Where s is the “loading harmonic order,” which can take on any integer value. One way to approach this new term is to assign different values to it and see how it affects k . We used a MATLAB routine called “Rotor_Stator.m” to implement this operation.

There is, as it turns out, a convenient way to circumvent the complication introduced by s . For a specific BPF tone of interest (a is given), we start off by varying m instead of a and s . Each BPF tone corresponds to a variety of s ; if the mode is evanescent for all s , we conclude that the acoustic wave is cut-off on that BPF tone. We adopt annular duct acoustics to calculate the cut-off frequencies F_m for an interval of m (we assume m is positive because a negative m indicates that the wave rotates contrary in the circumferential direction to that of the rotor). The exact cut-on (off) criterion is:

$$M_{ip} = \frac{Z_{mb}}{aB} \sqrt{(1-M^2)} \quad (18)$$

Consequently:

$$F_m = \frac{\omega}{2\pi} = \frac{Z_{mb}c}{2\pi} \sqrt{(1-M^2)} \quad (19)$$

We are mostly concerned about the first radial mode (i.e., $b = 1$), so we have acquired all the inputs for calculating Z_{mb} . On the BPF tone, if for a specific m (call it m^*) F_m^* is larger than the BPF tone frequency (Equation 20), i.e., if:

$$F_m^* > B\Omega / 2\pi \quad (20)$$

Then, the mode is cut-off on the BPF tone. Because F_m increases as m increases, all modes with m larger or equal to m^* would be cut-off on that BPF tone. Ultimately, the addition of stator simply provides us a method to achieve our sound-suppressing goal by cutting off the BPF tone through a sufficiently large vane count. In other words, for each BPF tone we have a variety of s ; as long as at least one of them yields a cut-on mode, the wave at that BPF frequency will propagate unattenuated.

Experimental Setup

The acoustic testing is carried out in UC Irvine’s Aeroacoustics Facility (Truong and Papamoschou, 2013). The anechoic chamber (Figure 4) houses twenty-four 3.2mm condenser microphones with a frequency response of 140 kHz. With different arrangements of the two arms containing the microphones, the recorded polar angle θ

ranges from 20° to 120° relative to the downstream rotor axis (Figure 5). The microphones are connected with six conditioning amplifiers. National Instruments LabView software is used to acquire the signals. The Sound Pressure Level Spectra are corrected for atmospheric absorption and free-field correction. The SPLs for different polar angles are plotted via MATLAB.

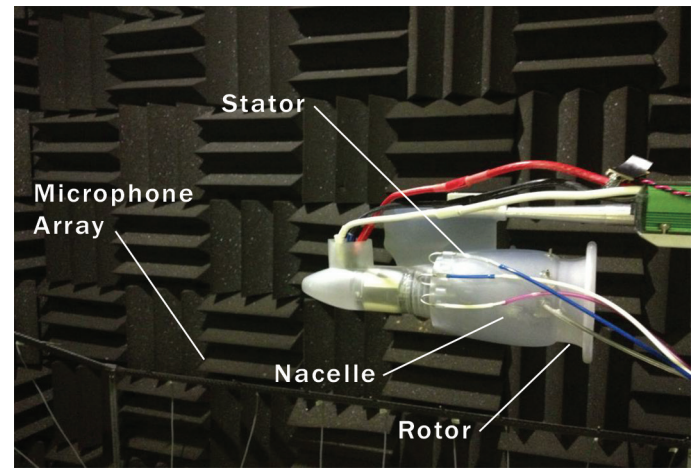


Figure 4
Inside look of the anechoic chamber

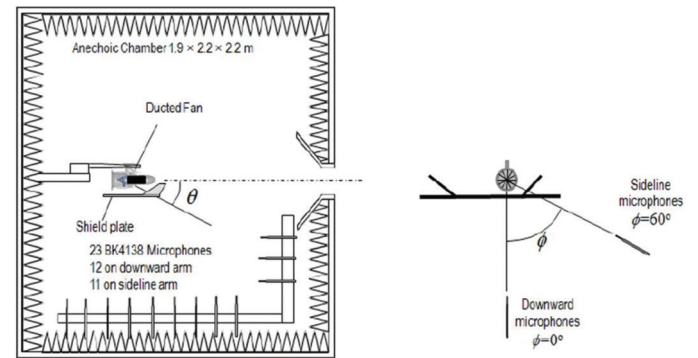


Figure 5
Microphone array and polar & azimuthal angle conventions. Source: Truong and Papamoschou (2013).

Results and Discussion

We used the specifications of the previously designed rotor to test the theory's validity ($B = 14$, $V = 24$, $R = 0.035\text{m}$, $q = 0.0152\text{m}$). For this example we chose the first two BPF tones, i.e., $a = 1$ and $a = 2$. The routine "Annular_Duct_With_Stator_New_Test.m" calculates the cut-off criterion for the second BPF tone to be 17.43; this is the eigenvalue above which the wave with corresponding m is cut-off. A matrix containing all the eigenvalues for an interval of m is

displayed. For $m = 15$, the eigenvalue approaches 17, so it is concluded that for m larger than 15, the acoustic wave is cut-off on the second BPF tone.

The azimuthal periodicity in the case of the second BPF tone is:

Second BPF: $m = 28 + 24s$, with $s = \dots -2, -1, 0, 1, 2, 3 \dots$

It follows that with $s = -1$ the wave is cut-on, so we expect a distinct peak for the second BPF tone for the sound pressure spectra.

Similarly, for the first BPF tone, the eigenvalue associated with cut-off (on) criterion is 8.72; this corresponds to $m = 6$. Therefore, for m larger than 6, the eigenvalue would exceed 8.72 and the mode would be cut-off. From the expression below, it is clear that for all possible s the wave would be cut-off; therefore, we should expect the first tone to be suppressed.

First BPF: $m = 14 + 24s$, with $s = \dots -2, -1, 0, 1, 2, 3 \dots$

To test this theoretical cut-off scenario, we run several acoustic tests of the GTF recorded on different polar angles; as the spectra suggests, it is almost always true for polar angles lower than 80° that the first BPF tone is less prominent than the second BPF tone, yet we do not witness complete removal of the first peak (Figure 6).

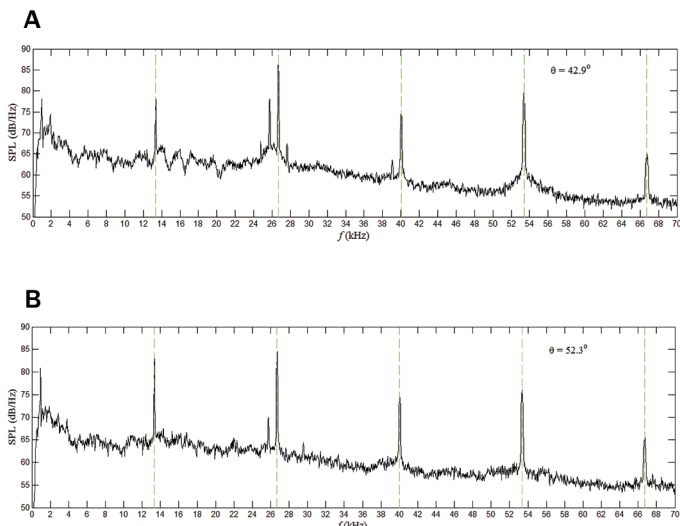


Figure 6
(A) SPL plotted at polar angle equal to 42.9 degrees. (B) SPL plotted at polar angle equal to 52.3 degrees.

However, when the polar angle goes above 75° , the sound pressure level associated with the first BPF tone always

exceeds that of the second tone (Figure 7). The physical mechanism behind this anomaly is still under investigation; yet, this issue can be resolved with proper shielding for the sake of real-world application, which proves to be particularly effective in suppressing acoustic modes with high polar angles. In addition, although the first BPF is restrained to a certain extent, we do not observe complete cut-off as the theory would predict; this mismatch partially stems from the infinite-duct assumption, as well as the fact that the stator vane count is not significantly larger than the blade count. In future investigations, we hope to construct stators with various vane counts to comprehensively and rigorously validate the theory.

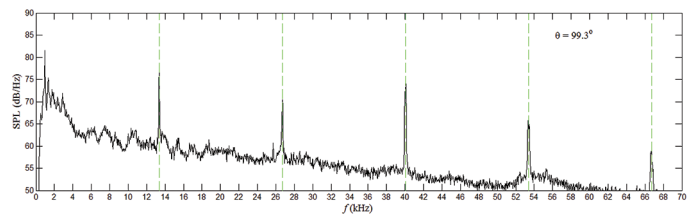


Figure 7
SPL plotted at θ equal to 99.3 degrees. With this high polar angle we observe a higher peak at the first BPF frequency than at the second.

Conclusion

Acoustics testing of the designed small-scale GTF suggests that it could successfully replicate the tonal noises generated by realistic GTF engines installed on airliners with good accuracy. During almost all the testing runs, the aerodynamic performance of the rotor was satisfactory and blade-stall situations were avoided. Although several rotors did break due to the blade tip coming in touch with the nacelle wall, few of these rotors were destroyed because of their inability to handle excessive centrifugal forces. This suggests the design of the rotor yields credible solidity, given that the rotational speed is extremely high (58,000 RPM). In addition, at reasonably low polar angles, the annular duct theory accurately predicts the cut-off scenario for the first BPF tone and the cut-on scenario for the second BPF tone. The developed cut-on (off) criterion needs to be modified further to accommodate the finite length of the fan duct.

In conclusion, future acoustic tests regarding GTF engines can be simulated using the very-small-scale GTF designed and fabricated in our Aeroacoustics Lab. This innovative apparatus could remarkably curb the cost of experiments, and still yield meaningful results regarding the acoustic testing of innovative sound-attenuation techniques.

Acknowledgements

I would like to thank my advisor, Dr. Dimitri Papamoschou, for taking me under his wing, squeezing time out of his compact schedule and patiently answering all the questions that I came up with; I cannot remember once that he refused to meet me due to his extremely busy schedule. Also, I would like to thank Alex Truong for his great assistance in helping me understand the design procedure of the rotor blade; he started from some of the most fundamental concepts and eventually guided me through the entire process. Vincent Phong, although he does not specialize in rotor design, generously helped me with fundamental aerodynamics concepts, which turned out to be very crucial. Also, to all of the former and current members of UC Irvine's Aeroacoustics Lab, thank you for your friendship and help.

Works Cited

- Alonso, Jose and Ricardo Burdisso. "Eigenvalue solution for the convected wave equation in a circular soft wall duct." *Journal of Sound and Vibration*. 315 (2008) 1003–1015.
- Ju, Hongbin. "Sound Propagation in Ducts." *Academia Search*. June 2012. Web. 6 January 2013.
- Rienstra, W. Sjoerd and A. Hirschberg. *An Introduction to Acoustics*. Eindhoven: Eindhoven University of Technology, 2004. Google Web Search. Web. 28 August 2013.
- Polacsek, C. John and F. Desbois-Lavergne. "Fan interaction noise reduction using a wake generator: experiments and computational aeroacoustics." *Journal of Sound and Vibration*. 265 (2003) 725–743.
- Truong, Alex, and Dimitri Papamoschou. "Aeroacoustic Testing of Open Rotors at Very Small Scale." AIAA-2013-0217, 51st AIAA Aerospace Sciences Meeting, Grapevine, TX, Jan. 7–10, 2013.
- Truong, Alex, and Dimitri Papamoschou. "GTF Experimental Details." *Internal report UC Irvine* (2013). Web. 7 August 2013.

